



Molecular Modeling on the Identification of Potential Janus Kinase 3 (JAK3) Inhibitors Based on the Indonesian Medicinal Plant Database

Muhammad Arba^{1*}, Sanang Nur Safitri¹, Andry-Nur Hidayat¹,
Arry Yanuar², Muhammad Sulaiman Zubair³, Asmiyenti Djaliasrin Djalil⁴ &
Daryono Hadi Tjahjono⁵

¹Faculty of Pharmacy, Universitas Halu Oleo, Kendari 93231, Indonesia

²Faculty of Pharmacy, Universitas Indonesia, Depok 16424, Indonesia

³Department of Pharmacy, Tadulako University, Palu, Indonesia

⁴Faculty of Pharmacy, Universitas Muhammadiyah Purwokerto, Purwokerto, Indonesia

⁵School of Pharmacy, Institut Teknologi Bandung,

Jalan Ganesha 10, Bandung 40132, Indonesia

E-mail: muh.arba@uho.ac.id

Abstract. The Janus tyrosine kinases (JAKs) have shown great promise as therapeutic protein targets in the treatment of cancer and inflammation diseases. This study used pharmacophore modeling to identify potential inhibitors of Janus kinase 3 (JAK3). A pharmacophore model was developed based on a known JAK3 inhibitor (1NX) and was employed to search for potential JAK3 inhibitors against Indonesian herbal compounds. Among 28 hit molecules that were identified and subjected to a molecular docking protocol against JAK3, the three compounds that had the highest affinities toward JAK3 were camelliaside B, 3-O-galloylepicatechin-(4beta-6)-epicatechin-3-O-gallate, and mesuaferrone B. These were then each subjected to a 50-ns molecular dynamics (MD) simulation. Analysis of RMSD and RMSF values indicated that the three compounds reached stability during the MD simulation. Interestingly, all three compounds had lower binding energies than 1NX against JAK3, as predicted by the MM-PBSA binding energy calculation.

Keywords: *Janus kinase; MM-PBSA; molecular dynamics simulation; pharmacophore modeling; virtual screening.*

1 Introduction

Janus kinases (JAKs) are members of the family of intracellular tyrosine kinases. They are phosphotransferases that bind to cytokine receptors, including interleukins, interferons, and many other cytokines [1]. Janus kinases, along with their signal transducer and activators of transcription proteins (STAT), mediate transduction of signaling cascades through the JAK-STAT-PI3K-MAPK pathway, which is crucial for the differentiation, proliferation and survival of a variety of cell types [2-5].

Received October 17th, 2019, Revised October 10th, 2020, Accepted for publication October 20th, 2020

Copyright © 2020 Published by ITB Institute for Research and Community Services, ISSN: 2337-5760,

DOI: 10.5614/j.math.fund.sci.2020.52.3.2

The JAK family consists of 4 isoforms, namely JAK1, JAK2, JAK3 and Tyk2. They have similar biochemical properties due to high sequence homologies. While JAK1, JAK2, and Tyk2 are predominantly found in a variety of cell types, JAK3 is chiefly expressed in hematopoietic, myeloid and lymphoid cells [6]. More specifically, JAK3 is limited to the gamma chain (γ c) subfamily of cytokines in both humans and mice [3,4,7,8]. Thus, inhibition of JAK3 is a promising approach for the elimination of autoimmune and inflammatory diseases [9]. Various JAK3 inhibitors have been researched, including tofacitinib and ruxolitinib [8,9]. However, several adverse effects, including increased risk of infection, lymphoma, cancer and tuberculosis, were noted in the clinical use of these inhibitors, which are attributable to the inhibition of multiple JAKs due to the high extent of structural conservation of the ATP binding site of JAK [1,3,4,10,11]. Thus, the search for more selective and potent JAK3 inhibitors is being actively pursued, both in academic institutions and pharmaceutical companies. Here we report a pharmacophore model of JAK3, which was used to screen the Indonesian Medicinal Plants Database (HerbalDB) [12]. Pharmacophore-based *in silico* screening was combined with a molecular docking simulation to identify novel potential JAK3 inhibitors from the Indonesian herbal database. Further, a molecular dynamics simulation was performed to confirm the stable interaction between the ligands and JAK3. Finally, the Molecular-Mechanics Poisson Boltzmann Surface Area (MM-PBSA) method was utilized to assess the affinity of the hit molecules.

2 Method

2.1 Structure-based Pharmacophore Modeling

A pharmacophore model was built by employing the structure of a carboxamide (INX) complexed with JAK3, which was retrieved from Research Collaboratory for Structural Bioinformatics PDB ID 3ZEP [13]. Validation of the pharmacophore model was conducted by performing screening against 100 actives taken from BindingDB [14] and 7500 decoys retrieved from the DUD-E database [15]. This task was completed by using the LigandScout Advanced 4.3 software [16]. The validated model was employed to identify potential inhibitors of JAK3 against the Indonesian Medicinal Plants Database (HerbalDB) [12], which contains 1379 molecules.

2.2 Molecular Docking, Molecular Dynamics and MM-PBSA Energy Calculation

The obtained hit molecules from pharmacophore screening were then subjected to molecular docking simulation to the JAK3 protein. A set of polar hydrogens was added and Kollman charges were assigned to the JAK3 in the receptor

preparation step. This task was performed using AutoDockTools 1.5.6. Each ligand was then docked into an active site of JAK3, which was established based on the grid box, which was the center of the native ligand (1NX) coordinates. The molecular docking was carried out by using the iDock software [17]. Each docked ligand conformation was analyzed and visualized using Discovery Studio Visualizer 2016 and the three molecules with the best binding affinities and with good interaction were subjected to a molecular dynamics simulation.

The molecular dynamics simulation was performed for each four ligands complexed with JAK3 employing the AMBER16 package [18-21]. The leap module was used to prepare each complex using the ff14SB force field [22] for the protein and the GAFF force field [23], and AM1-BCC [24] for the ligands. The protein was protonated according to the default Amber procedure. The minimization, heating and equilibration steps, the MM-PBSA calculation and the parameters employed are described in our previous publication [21]. The production MD simulation was conducted for 50 ns in NPT ensemble [21].

3 Results and Discussion

The structure of a carboxamide (1NX) complexed with JAK3 was adopted for building the pharmacophore model, which resulted in several pharmacophore models. From these models, one hypothesis was found, consisting of one hydrogen bond (H-bond) acceptor, two H-bond donors, and two hydrophobic features. Figure 1 shows the generated pharmacophore model.

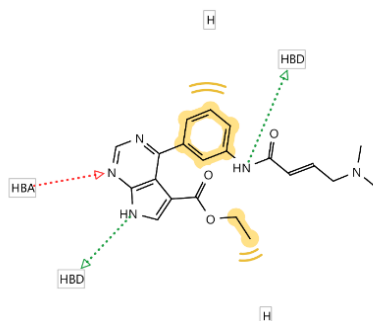


Figure 1 3D pharmacophore model, consisting of one H-bond acceptor (red dotted lines), two H-bond donors (green dotted lines), and two hydrophobic (yellow sphere) features.

The pharmacophore model was then validated against 100 actives and 7500 decoys. It was found that the area under curve (AUC) of the receiver operating characteristic (ROC) curve was 0.52. Meanwhile the calculation of the goodness

of hit score (GH score) gave a result of 0.76. Both parameters indicated the validity of the pharmacophore model developed. Figure 2 displays the AUC of the ROC curve.

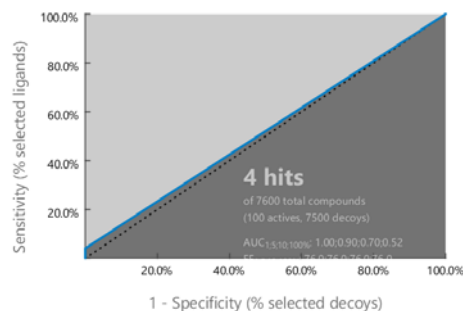


Figure 2 The AUC plot of the ROC curve.

Screening for hit molecules against the Indonesian Herbal Database (HerbalDB) yielded 28 hit molecules. Molecular docking of each hit molecule into JAK3 gave binding energies between -7.52 and -9.97 kcal/mol. These energy values are comparable to the binding energy of a docked native ligand (INX) of -8.82 kcal/mol. Further, we selected the three best docked hit molecules for an MD simulation, i.e. camelliaside B/Lig2 ($E = -9.97$ kcal/mol), 3-O-galloylepicatechin-(4beta-6)-epicatechin-3-O-gallate/lig 10 ($E = -9.91$ kcal/mol), and mesuaferone B/Lig17 ($E = -9.74$ kcal/mol). Figure 3 shows the hit structures of the three best docked hit molecules.

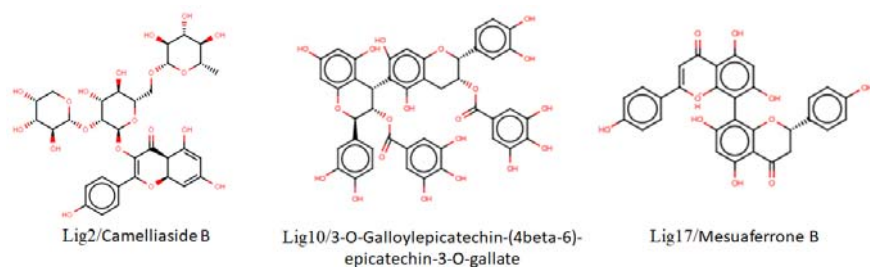


Figure 3 The hit structures of the three best docked hit molecules.

Binding conformations of the hit molecules occurred in the binding site of JAK3. Lig2 formed five H-bond interactions with Lys830, Cys909, Arg911, Asp967, and Arg953, while Lig10 formed H-bond interactions with Lys855, Leu905, Glu903, Lys830, Asp912, Met902, and Gln827. The binding of Lig17 was also corroborated with H-bonds Cys909, Asp967, and Leu905. Amino acid residue Cys909 is known as a key active site residue of JAK3. Figure 4 depicts the binding interactions of each ligand within the binding pocket of JAK3.

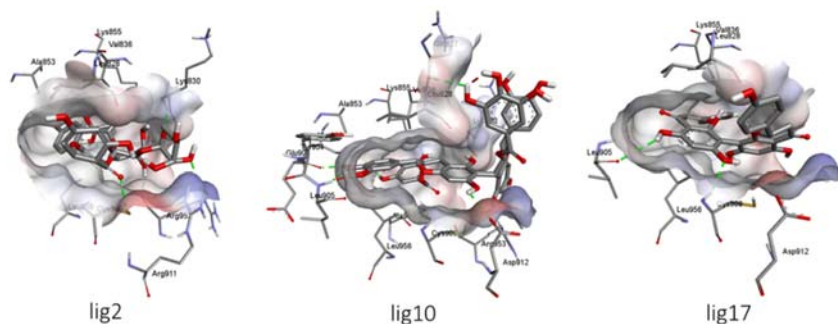


Figure 4 The binding interactions of Lig2, Lig10 and Lig17 within the binding pocket of JAK3.

3.1 Molecular Dynamics Simulations

As the molecular docking method does not consider the physiological condition for stable interaction of the hit molecules, each three best docked hit molecules complexed with JAK3 were subjected to an MD simulation. The MD simulation was carried out for 50 ns to see whether the ligands would retain interaction with JAK3. The values of root mean square deviation (RMSD) during the MD simulation run were used to monitor the stability of the complex. Figure 5 shows the RMSD values of the heavy atoms ($C\alpha$, C, N, O) of JAK3.

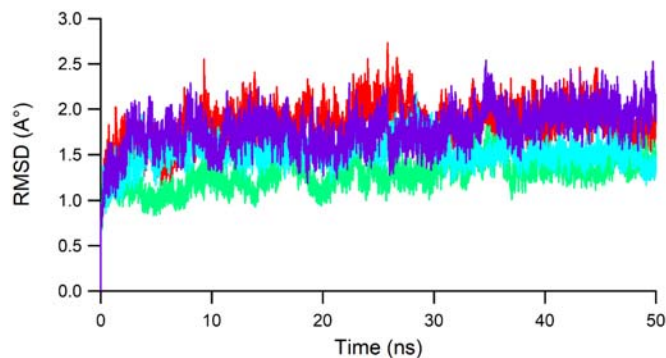


Figure 5 The RMSD values of the main protein atoms of each JAK3 ligand system during 50 ns MD accounted for Lig2, Lig10, Lig17, and 1NX, colored red, green, blue, and purple, respectively.

It is noted that each ligand maintained stable interaction with JAK3. Lig10 (green) and Lig17 (blue) had lower RMSD values than 1NX, which indicates more stable interactions. All fluctuations of the RMSD values for all ligands were under 3 Å, which can be considered stable conformational changes, during 50 ns.

The fluctuation of the individual amino acid residues during the MD simulation was recorded as a root mean square fluctuation (RMSF) plot. Figure 6 displays the RMSF values for the individual amino acids during 50 ns.

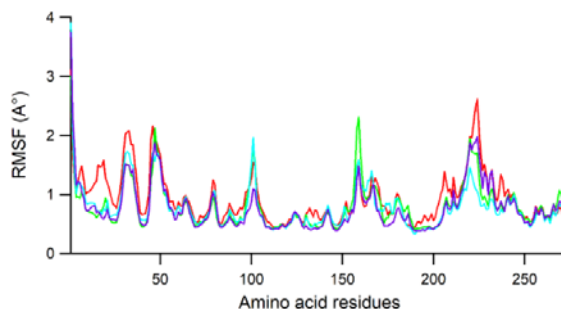


Figure 6 Plot of RMSF for Lig2, Lig10, Lig17 and 1NX, colored red, green, blue, and purple, respectively.

The same pattern of amino acid fluctuation was noted in the whole region of JAK3, which indicates the same binding interaction of the ligands. Overall, the amino acid residues fluctuated under 3 Å, except for those composing the carboxy and amino ends of the protein, which indicates stable dynamics during 50 ns. Dominant peaks were recorded in the residues of around Asp33 (Asp846), HisS46 (His859), Ala101 (Ala919), Asp159 (Asp977), which corresponds to loop regions. The higher peak at Ser224 (Ser1048) is associated with the end of a helix. On the other hand, the amino acid residues involved in the H-bond interactions over all ligands, including Cys91 (Cys909), showed more rigid fluctuation, which indicates protein stability induced by ligand interactions.

Meanwhile, several H-bond interactions of docked conformations were also retained in the MD simulation. For example, H-bonds between Lig2 and JAK3 occurred with occupancies of 45.73%, 26.81%, 16.04%, and 15.72%, with the residues of Arg953 (Arg135), Arg911 (Arg93), Lys830 (Lys17), and Asp967 (Asp149), respectively. Newly formed H-bond interactions with very high occupancies (97.31 and 90.8%) were recorded, namely with Glu871 (Glu58) and Glu85 (Glu903), respectively. On the other hand, Lig10 retained H-bond interactions with Asp912 (Asp94), Lys830 (Lys17), Glu903 (Glu85), Leu905 (Leu87), Gln827 (Gln14) and Lys855 (Lys42), with occupancies of 44.89%, 39.04%, 37.86%, 28.39, 21.54% and 17.36%, respectively. Newly formed H-bond interactions with very high occupancy (71.04 %) were recorded with Glu871 (Glu58) and with moderate occupancy (51.9%) with Arg953 (Arg135). The binding of Lig17 maintained H-bond interaction with Asp967 (Asp149) with 75.72% occupancy, and novel H-bonds were maintained with Arg953

(Arg135) and Asp912 (Asp94) with 88.25% and 54.88% occupancy, respectively. Table S1 shows the H-bond occupancies recorded during the 50-ns simulation.

3.2 Free Binding Energy Calculations

The stable conformation of ligands during the MDs simulation run was then subjected to the MM-PBSA protocol for free binding energy prediction. Prediction of binding energy using the MM-PBSA method is widely considered as more accurate compared to using the docking method. Table 1 shows the calculated binding affinities from the MM-PBSA method. Interestingly, the free binding energies of Lig2 ($\Delta E_{\text{PBTOT}} = -19.35 \pm 7.16$), Lig10 ($\Delta E_{\text{PBTOT}} = -26.55 \pm 8.13$), and Lig17 ($\Delta E_{\text{PBTOT}} = -25.34 \pm 3.94$) were more negative than that of 1NX (-16.90 ± 3.04). The binding energy of Lig17 appeared to be most negative among them. Negative binding free energy originating from favorable electrostatic, van der Waals as well as non-polar energies contributes to the solvation energy.

Table 1 MM-PBSA free binding energy for each ligand.

Ligand	ΔE_{ELE} (kcal/mol)	ΔE_{VDW} (kcal/mol)	ΔE_{PBCAL} (kcal/mol)	ΔE_{PBSUR} (kcal/mol)	ΔE_{PBTOT} (kcal/mol)
1NX	-67.65 ± 11.09	-30.53 ± 2.68	85.07 ± 10.94	-3.81 ± 0.20	-16.90 ± 3.04
Lig2	-59.40 ± 13.19	-49.07 ± 5.09	94.70 ± 8.69	-5.58 ± 0.23	-19.35 ± 7.16
Lig10	-91.14 ± 11.90	-57.84 ± 5.10	128.89 ± 15.77	-6.46 ± 0.22	-26.55 ± 8.13
Lig17	-55.88 ± 7.25	-44.37 ± 3.48	79.91 ± 7.20	-5.00 ± 0.13	-25.34 ± 3.94

4 Conclusion

Structure-based pharmacophore modelling was performed based on JAK3-1NX interaction. A pharmacophore hypothesis was built and validated. It was then used to identify hit molecules in the Indonesian Herbal Database. Twenty-eight hit molecules were retrieved and then docked into the active site of JAK3 to reveal their binding interactions. The hit molecules maintained their interactions with the JAK3 through H-bond and hydrophobic interactions. The three best hits, i.e. camelliaside B, 3-O-galloylepicatechin-(4beta-6)-epicatechin-3-O-gallate, and mesuaferrone B, were subjected to an MD simulation, which showed good stability during 50 ns. Prediction of binding affinities using the MM-PBSA method showed that the three top hit molecules displayed stronger affinities than 1NX. The contribution of the van der Waals, electrostatic and nonpolar energies to the solvation energy interactions were favorable for most of the three molecules. The present work suggests that these three molecules may serve as potential inhibitors of JAK3.

Acknowledgement

Authors sincerely thanks the Ministry of Research and Technology Republic of Indonesia for its partial funding provided through grant PDUPT, 2020.

References

- [1] O'Shea, J.J. & Gadina, M., *Selective Janus Kinase Inhibitors Come of Age*, Nat Rev Rheumatol, **15**(2), pp. 74-75, 2019.
- [2] Wang, Y., Huang, W., Xin, M., Chen, P., Gui, L., Zhao, X., Zhu, X., Luo, H., Cong, X., Wang, J. & Liu, F., *Discovery of Potent Anti-inflammatory 4-(4,5,6,7-tetrahydrofuro[3,2-c]pyridin-2-yl) pyrimidin-2-amines for Use as Janus Kinase Inhibitors*, Bioorg. Med. Chem., **27**(12), pp. 2592-2597, 2019.
- [3] Yu, R-N., Chen, C-J., Shu, L., Yin, Y., Wang, Z-J., Zhang, T-T., & Zhang, D-Y., *Structure-based Design and Synthesis of Pyrimidine-4,6-diamine Derivatives as Janus Kinase 3 Inhibitors*, Bioorg. Med. Chem., **27**(8), pp. 1646-1657, 2019.
- [4] Yin, Y., Chen, C-J., Yu, R-N., Wang, Z-J., Zhang, T-T. & Zhang, D-Y., *Structure-based Design and Synthesis of 1H-pyrazolo[3,4-d]pyrimidin-4-amino Derivatives as Janus Kinase 3 Inhibitors*, Bioorg. Med. Chem., **26**(17), pp. 4774-4786, 2018.
- [5] Wu, W. & Sun, X-H., *Janus Kinase 3: The Controller and The Controlled*, Acta Biochim. Biophys. Sin. (Shanghai), **44**(3), pp. 187-196, 2011.
- [6] Shi, L., Zhong, Z., Li, X., Zhou, Y. & Pan, Z., *Discovery of an Orally Available Janus Kinase 3 Selective Covalent Inhibitor*, J. Med. Chem., **62**, pp. 1054-1066, 2019.
- [7] Su, D., Gao, Y., Deng, Y., Zhang, H., Wu, Y., Hu, Y. & Mei, Q., *Identification of Chinese Herbal Compounds with Potential as JAK3 Inhibitors*, Evid. Based Complement Alternat. Med., **2019**, pp. 1-11, 2019.
- [8] Tan, L., Akahane, K., McNally, R., Reyskens, K.M.S.E., Ficarro, S.B., Liu, S., Herter-Sprrie, G.S., Koyama, S., Pattison, M.J., Labella, K., Johannessen, L., Akbay, E. A., Wong, K-K., Frank, D.A., Marto, J.A., Look, T.A., Arthur, J.S.C., Eck, M.J. & Gray, N.S., *Development of Selective Covalent Janus Kinase 3 Inhibitors*, J. Med. Chem., **58** (16), pp. 6589-6606, 2015.
- [9] Norman, P., *Highly Selective Janus Kinase 3 Inhibitors based on a Pyrrolo[2,3-d]pyrimidine Scaffold: Evaluation of WO2013085802*, Expert Opin. Ther. Pat., **24** (1), pp. 121-125, 2014.
- [10] Jasuja, H., Chadha, N., Singh, P.K., Kaur, M., Bahia, M.S. & Silakari, O., *Putative Dual Inhibitors of Janus Kinase 1 and 3 (JAK1/3):*

- Pharmacophore Based Hierarchical Virtual Screening*, *Comput. Biol. Chem.*, **76**, pp. 109-117, 2018.
- [11] Tan, L., Akahane, K., McNally, R., Reyskens, K.M.S.E., Ficarro, S.B., Liu, S., Herter-Sprue, G.S., Koyama, S., Pattison, M.J., Labella, K., Johannessen, L., Akbay, E. A., Wong, K.K., Frank, D.A., Marto, J.A., Look, T.A., Arthur, J.S.C., Eck, M.J. & Gray, N.S., *Development of Selective Covalent Janus Kinase 3 Inhibitors*, *J. Med. Chem.*, **58** (16), pp. 6589-6606, 2015.
- [12] Yanuar, A., Mun'im, A., Lagho, A.B.A., Syahdi, R.R., Rahmat, M. & Suhartanto, H., *Medicinal Plants Database and Three Dimensional Structure of the Chemical Compounds from Medicinal Plants in Indonesia*, *Int. J. Comput. Sci.*, **8**(5), pp. 180-183, 2011.
- [13] Jaime-Figueroa, S., De Vicente, J., Hermann, J., Jahangir, A., Jin, S., Kuglstatter, A., Lynch, S. M., Menke, J., Niu, L., Patel, V., Shao, A., Soth, M., Vu, M.D. & Yee, C., *Discovery of a Series of Novel 5H-Pyrrolo[2,3-B]Pyrazine-2-Phenyl Ethers, as Potent JAK3 Kinase Inhibitors*, *Bioorganic Med. Chem. Lett.*, **23**(9), pp. 2522-2526, 2013.
- [14] Gilson, M.K., Liu, T., Baitaluk, M., Nicola, G., Hwang, L. & Chong, J., *BindingDB in 2015: A Public Database for Medicinal Chemistry, Computational Chemistry and Systems Pharmacology*, *Nucleic Acids Res.*, **44**, pp. 1045-1053, 2016.
- [15] Mysinger, M.M., Carchia, M., Irwin, J.J. & Shoichet, B. K., *Directory of Useful Decoys, Enhanced (DUD-E): Better Ligands and Decoys for Better Benchmarking*, *J. Med. Chem.*, **55**(14), pp. 6582-6594, 2012.
- [16] Wolber, G. & Langer, T., *LigandScout: 3-D Pharmacophores Derived from Protein-Bound Ligands and their Use as Virtual Screening Filters*, *J. Chem. Inf. Model*, **45**(1), pp. 160-169, 2005.
- [17] Li, H., Leung, K. & Wong, M., *Idock: A Multithreaded Virtual Screening Tool for Flexible Ligand Docking*, 2012 IEEE Symposium on Computational Intelligence in Bioinformatics and Computational Biology (CIBCB), pp. 77-84, 2012.
- [18] Case, D.A., Cheatham, T.E., Darden, T., Gohlke, H., Luo, R., Merz, K.M., Onufriev, A., Simmerling, C., Wang, B. & Woods, R.J., *The AMBER Biomolecular Simulation Programs*, *J. Comput. Chem.*, **26**(16), pp. 1668-1688, 2005.
- [19] Salomon-Ferrer, R., Götz, A. W., Poole, D., Le Grand, S. & Walker, R.C., *Routine Microsecond Molecular Dynamics Simulations with AMBER on Gpus. 2. Explicit Solvent Particle Mesh Ewald*, *J. Chem. Theory Comput.*, **9**(9), pp. 3878-3888, 2013.
- [20] Arba, M., Ruslin, Kalsum, W.U., Alroem, A., Muzakkar, M.Z., Usman, I. & Tjahjono, D.H., *QSAR, Molecular Docking and Dynamics Studies of Quinazoline Derivatives as Inhibitor of Phosphatidylinositol 3-Kinase*, *J. Appl. Pharm. Sci.*, **8**(5), pp. 1-9, 2018.

- [21] Arba, M. & Nur-Hidayat, A., Surantaadmaja, S.I. & Tjahjono, D.H., *Pharmacophore-Based Virtual Screening for Identifying B5 Subunit Inhibitor of 20S Proteasome*, *Comput. Biol. Chem.*, **77**, pp. 64-71, 2018.
- [22] Maier, J.A., Martinez, C., Kasavajhala, K., Wickstrom, L., Hauser, K.E. & Simmerling, C., *ff14SB: Improving the Accuracy of Protein Side Chain and Backbone Parameters from ff99SB*, *J. Chem. Theory Comput.*, **11**(8), pp. 3696-3713, 2015.
- [23] Wang, J.M., Wolf, R.M., Caldwell, J.W., Kollman, P.A. & Case, D.A., *Development and Testing of a General Amber Force Field*, *J. Comput. Chem.*, **25**(9), pp. 1157-1174, 2004.
- [24] Jakalian, A., Jack, D.B. & Bayly, C.I., *Fast, Efficient Generation of High-Quality Atomic Charges. AM1-BCC Model: II. Parameterization and Validation*, *J. Comput. Chem.*, **23**(16), pp. 1623-1641, 2002.
- [25] Ryckaert, J.P., Ciccotti, G. & Berendsen, H.J.C., *Numerical Integration of the Cartesian Equations of Motion of a System with Constraints: Molecular Dynamics of N-Alkanes*, *J. Comput. Phys.*, **23**(3), pp. 327-341, 1977.
- [26] Darden, T., York, D. & Pedersen, L., *Particle mesh Ewald: An N-log(N) Method for Ewald Sums in Large Systems*, *J. Chem. Phys.*, **98**(12), pp. 10089-10092, 1993.
- [27] Roe, D.R. & Cheatham III, T.E., *PTRAJ and CPPTRAJ: Software for Processing and Analysis of Molecular Dynamics Trajectory Data*, *J. Chem. Theory Com.*, **9**(7), pp. 3084-3095, 2013.
- [28] Humphrey, W., Dalke, A. & Schulten, K., *VMD: Visual Molecular Dynamics*, *J. Mol. Graph.*, **14**(1), pp. 33-38, 1996.
- [29] Kollman, P.A., Massova, I., Reyes, C., Kuhn, B., Huo, S., Chong, L., Lee, M., Lee, T., Duan, Y., Wang, W., Donini, O., Cieplak, P., Srinivasan, J., Case, D.A. & Cheatham, T.E., *Calculating Structures and Free Energies of Complex Molecules: Combining Molecular Mechanics and Continuum Models*, *Acc. Chem. Res.*, **33**(12), pp. 889-897, 2000.
- [30] Miller, B.R., McGee, T.D., Swails, J. M., Homeyer, N., Gohlke, H. & Roitberg, A.E., 2012, *MMPBSA.py: An efficient Program for End-State Free Energy Calculations*, *J. Chem. Theory Comput.*, **8**(9), 3314-3321, 2012.
- [31] Arba, M., Yamin, Ihsan, S. & Tjahjono, D.H., *Computational approach Toward Targeting the Interaction of Porphyrin Derivatives with Bcl-2*, *J Appl. Pharm. Sci.*, **8**(12), pp. 60-66, 2018.
- [32] Arba, M., Ruslin, Ihsan, S., Tri Wahyudi, S. & Tjahjono, D.H., *Molecular Modeling of Cationic Porphyrin-Anthraquinone Hybrids as DNA Topoisomerase II β Inhibitors*, *Comput. Biol. Chem.*, **71**, pp. 129-135, 2017.